Electrocatalysis manuscript No.
(will be inserted by the editor)

Methanol oxidation on Pt(111) from first-principles in heterogeneous and electro-catalysis

Sung Sakong · Axel Groß

the date of receipt and acceptance should be inserted later

Abstract The catalytic oxidation of methanol on Pt(111) has been addressed based on first-principles electronic structure calculations. The chemical environment corresponding to the conditions in heterogeneous and electro-catalysis has been taken into account in a grand-canonical approach. Furthermore, the aqueous electrolyte in electrocatalysis has been described in an implicit solvent model. Thus we find characteristic differences between the methanol oxidation paths in heterogeneous and electro-catalysis. The presence of the aqueous electrolyte stabilizes reaction intermediates containing hydrophilic groups thus also influencing the selectivity in the methanol oxidation. In addition, adsorbed hydrogen on Pt(111) is shown to render the electro-oxidation of methanol less efficient.

1 Introduction

Reactions at electrochemical interfaces play an increasingly important role in devices for chemical energy conversion and storage [1]. This is reflected in a growing number of theoretical studies addressing electrode/electrolyte interfaces from first-principles [2–23] on the basis of periodic density functional theory (DFT) calculations. Electrocatalytic processes occur at the electrode/electrolyte interface. For a proper theoretical description of these reactions, it is critical to take into account the explicit structure of this interface [16, 19] which is governed by the species present in the electrolyte. Furthermore, the liquid nature of the electrolyte requires a numerically demanding statistical averaging over many possible configurations [2, 24] in order to derive free energies rather than total energies. However, because of limited computer

Sung Sakong
Institute of Theoretical Chemistry, Ulm University, 89069 Ulm, Germany

Axel Groß
Institute of Theoretical Chemistry, Ulm University, 89069 Ulm, Germany

power, first-principles calculations are still computationally too expensive to perform such statistical averages on a routine basis. As an attractive alternative, the influence of the electrolyte on structures and processes at electrochemical interfaces might be described in a grand-canonical approach with the species present in the electrolyte represented through their (electro-)chemical potential.

In the field of heterogeneous catalysis where reactions typically occur at the gas/solid-interface, this grand-canonical approach has been coined ab initio thermodynamics [25,26]. Usually the gas phase is not explicitly modeled but treated as a thermodynamic reservoir. The thermodynamic conditions just enter through the dependence of the chemical potentials of the atomic species on temperature, pressure, concentration, etc. Thus, e.g., the structure of metal catalysts in oxidation catalysis as a function of CO and oxygen partial pressure and temperature could be determined from first principles [27].

The concept of combining atomistic first-principles calculations with a grand-canonical approach to describe the environment was extended by Nørskov *et al.* to address the electrochemical environment characterized by the electrode potential and the concentrations of the species solvated in the electrolyte [28–31]. This method is now called the "computational hydrogen electrode".

Chemical reactions in heterogeneous catalysis occur at solid/gas interfaces, whereas the electrochemical reactions in electrocatalysis occur at solid/liquid interfaces. In heterogeneous catalysis, therefore, it is natural for reaction intermediates to refer their adsorption energy to free gas molecules. However, in electrocatalysis, the reference species correspond charged particles or ions in solution. To compute the energetics of these states again in principle require to calculate solvation energies on the basis of numerically very demanding thermodynamic integration schemes [32]. However, these expensive calculations can be avoided realizing the fact that typically solvated species are related to corresponding gaseous species given by standard electrode potentials. For example, the hydrogen electrochemical potential for a given electrode potential U can be expressed as

$$\tilde{\mu}_{\mathrm{H^+}} + \tilde{\mu}_{\mathrm{e^-}} = \frac{1}{2}\mu_{\mathrm{H_2}} - eU_{\mathrm{SHE}} - k_B T \ln(10)\mathrm{pH} \; . \tag{1}$$

where one has used the fact that at standard conditions defining the standard hydrogen electrode (SHE) potential U_{SHE} the solvated proton is in equilibrium with the H_2 molecule in the gas phase. The entropic contribution of varying proton concentration $-k_{\mathrm{B}}T\ln(10)p\mathrm{H}$ corresponds to a shift of about 59 meV in the electrochemical potential at room temperature if pH is changed by one. Thus, the computational hydrogen electrode method offers a convenient way to replace the reference energy of solvated ionic species by the reference energy of gaseous molecules.

In studies based on the concept of the computational hydrogen electrode, often the influence of the presence of the electrolyte on the energetics of the adsorbed system is neglected [29,15,19] which can be justified by the relatively

weak interaction of water with metal electrodes and simple adsorbates [33,34, 14]. However, the concept of computational hydrogen electrode allows to take the effect of the environment on adsorption energies into account. Still, as mentioned above, considering the presence of an aqueous electrolyte explicitly is prohibitively computationally expensive.

As a numerically attractive alternative, the electrolyte can be described as a dielectric continuum, i.e., in an implicit solvent model [35–38]. Recently we have used this approach to derive the equilibrium coverage of Pt(111) with hydrogen and OH as a function of the electrode potential [14]. Furthermore, we have addressed the methanol electro-oxidation on Pt(111) which is crucial process occurring on the anode of the direct methanol fuel cell (DMFC) [39,40]. We demonstrated that the presence of the aqueous electrolyte has a decisive influence on the selectivity within the reaction scheme [16] at an electrode potential of $U = 0.6\,\mathrm{V}$, at which Pt(111) is not covered by neither hydrogen nor OH and at which CO_2 formation becomes thermodynamically stable.

In this study, we will extend this previous study [16] by establishing a comparable scheme valid for the methanol oxidation in heterogeneous catalysis. By performing a detailed comparison of the reaction scheme of methanol oxidation in heterogeneous and electro-catalysis, we will gain a better understanding of the role of the electrochemical environment on electro-catalytic processes. Furthermore, we will also consider methanol electro-oxidation at lower electrode potential at which Pt(111) electrode is covered by protons, thus assessing the influence of adsorbates on the reaction energetics in methanol oxidation.

2 Computational details

Periodic DFT calculations have been performed using the software package VASP [41]. The exchange-correlation energies are evaluated within the generalized gradient approximation as suggested by Hammer and Nørskov, known as a revised version of the Perdew-Burke-Ernzerhof (RPBE) functional [42]. Dispersion effects have been considered within the semi-empirical D3 dispersion correction scheme of Grimme using the zero damping function [43–45]. The RPBE-D3 approach correctly predicts properties of liquid water [46,47, 17]. In addition, it reliably describes the interaction of organic molecules [48, 16] and water [46,47,17] with metal surfaces. The liquid electrolyte is modeled by a polarizable dielectric continuum as implemented into the VASP code by Mathew and Hennig [49,14]. Thus the thermally averaged contribution of electrolyte is effectively included in the DFT calculations yielding solvation energies and the local potential [35–38].

The wave functions were expanded up to a cutoff energy of 700 eV using a plane wave basis set to describe the solvation cavity accurately. The electronic cores are described by the projector augmented wave method [50]. The Pt lattice parameter of $a = 3.99\,\text{Å}$ is optimized using a fine k-point grid of $21 \times 21 \times 21$. The Pt catalyst is modeled by a Pt(111) slab consisting of five atomic layers. The top three layers of the slabs are fully relaxed, while the lower

most two layers are fixed at their bulk positions. The slabs are separated by a vacuum of 15 Å to avoid any interaction between the periodic images. The energetics of the reaction intermediates and barriers have been determined within a 3×3 surface super cell employing a $5 \times 5 \times 1$ k-point grid to integrate over the first Brillouin zone.

The cutoff radius for the pair interactions of D3 correction has been chosen to be 10 Å. However, the screening of the van der Waals interactions in bulk metals is not correctly described in dispersion correction schemes [46,51]. Therefore we exclude the dispersion correction for all metal atoms below the first layer.

The properties of liquid water are described with a dielectric constant of $\epsilon_b = 80$ and a cutoff charge density of $\rho_{\mathrm{cut}} = 0.0025\,\text{Å}^{-3}$. The cavitation energies are calculated using a surface tension parameter of $0.525\,\mathrm{meV/Å^2}$ [52] as described in Ref. [53,54]. The energies and forces of stable configurations satisfy the convergence criteria of 10^{-6} eV and $0.01\,\mathrm{eV/Å}$.

In the calculations, we will treat the chemical potential as a free parameter. The dependence of the reaction energetics on the thermodynamic conditions then enter through the corresponding dependence of the chemical potentials. Thus, the energetics of a given atomic adsorption configuration is given by the formation enthalpy

$$\Delta H = E_{tot} - \sum_i n_i \mu_i \tag{2}$$

with the total energy E_{tot}, chemical potential μ_i, and the number n_i of atomic species i per unit cell.

3 Chemical and electrochemical environments

As a first step in a grand-canonical simulation, the proper thermodynamic reservoirs of stable species have to be defined. The elements that are involved in the chemical reactions are carbon, hydrogen and oxygen. The specific reservoirs employed in this study are specified in Table 1. Let us first concentrate on the approach appropriate for the conditions in heterogeneous catalysis. Reactions in heterogeneous catalysis typically occur at the solid/gas interfaces. Therefore, the reference of the considered chemical species corresponds to gas-phase molecules. Let us consider the total oxidation of methanol on Pt(111)

Table 1 The selection of (electro-)chemical potentials in methanol oxidation heterogeneous catalysis and electrocatalysis.

	Heterogeneous Catalysis chemical potential μ	Electrocatalysis electrochemical potential $\tilde{\mu}$
carbon	$E_{\mathrm{CH_3OH(g)}} - 2E_{\mathrm{H_2O(g)}} + \mu_{\mathrm{O}}$	$E_{\mathrm{CH_3OH(aq)}} - E_{\mathrm{H_2O(aq)}} - 2\tilde{\mu}_{\mathrm{H^+}}$
hydrogen	$(E_{\mathrm{H_2O(g)}} - \mu_{\mathrm{O}})/2$	$\tilde{\mu}_{\mathrm{H^+}}$ (Eq. 1)
oxygen	$\mu_{\mathrm{O}}[p_{\mathrm{O_2(g)}}, T]$	$E_{\mathrm{H_2O(aq)}} - 2\tilde{\mu}_{\mathrm{H^+}}$

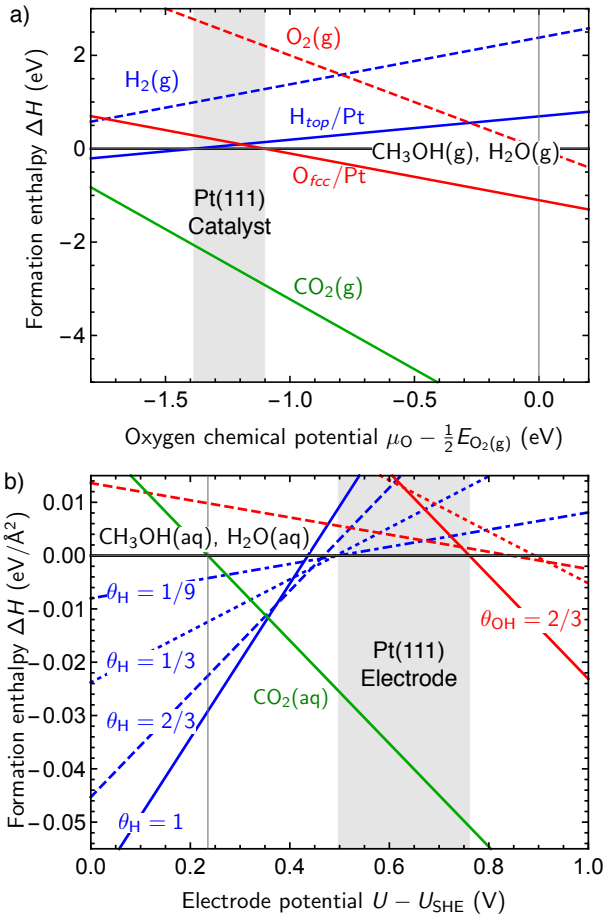

Fig. 1 a) Formation enthalpies of selected molecules and adsorbates in heterogeneous catalysis are displayed as a function of oxygen chemical potential at the chemical equilibrium between methanol and water molecules. Hydrogen and oxygen adsorption energies have been determined at a coverage of 1/9. b) Formation enthalpies of intrinsic H and OH species in electrocatalysis at the electrode/electrolyte interface are plotted as a function of electrode potential with respect to the standard hydrogen electrode, aqueous methanol, and aqueous water.

which can be expressed as

$$2\mathrm{CH_3OH(g)} + 3\mathrm{O_2(g)} \rightarrow 2\mathrm{CO_2(g)} + 4\mathrm{H_2O(g)}\ . \tag{3}$$

Specifically, for the heterogeneous catalysis situation we refer C and H to gas-phase methanol and water, respectively.

In practice, we will treat the chemical potential of O species μ_O as the control parameter. The chemical potential is related to the partial pressure and temperature of an $\mathrm{O_2}$ gas. Then, the formation enthalpy calculated by Eq. 2 becomes a function of μ_O as shown in Fig. 1a. Note that we relate the

hydrogen chemical potential to gas phase water so that according to Table 1 so that the chemical potential of hydrogen becomes a function of the chemical potential of oxygen.

Now we specify a range of oxygen chemical potentials that is beneficial for methanol oxidation. First of all we want to avoid any adsorbed hydrogen on Pt(111) in order to prevent any back reaction towards methanol. Thus under operating conditions, according to Fig 1a the chemical potential of oxygen should be larger than $-1.4\,\mathrm{eV}$. Second, the adsorption of oxygen on the surface leading to a passivation and a possible oxidation of the catalyst should also be avoided, leading to an upper bound of $-1.1\,\mathrm{eV}$ for the oxygen chemical potential. The favorable range of $-1.4 < \mu_\mathrm{O} < -1.1\,\mathrm{eV}$ is illustrated by the shaded area in Fig. 1a.

The chemical potential can be adjusted by changing the temperature and/or the partial pressure of dioxygen gas [55–57]. Assuming conditions of an ideal gas [58–60], at 700 K, the operating conditions correspond to a range of oxygen partial pressures of $10 < p_{\mathrm{O_2(g)}} < 10^5\,\mu\mathrm{Pa}$.

In contrast to heterogeneous catalysis, in electrocatalysis reactions occur at the solid electrode/liquid electrolyte interfaces. The reference states of the considered chemical species usually correspond to ions solvated in the electrolyte. The relevant overall reaction in methanol electro-oxidation can be expressed as

$$\mathrm{CH_3OH(aq) + H_2O(aq) \rightleftharpoons CO_2(aq) + 6H^+ + 6}e\ . \tag{4}$$

In order to establish the electrochemical environment, we select as the stable species in the grand-canonical reservoir solvated methanol and protons and aqueous water according to Table 1. The crucial parameter electrode potential enters the formalism through the electrochemical potential of solvated protons as shown in Eq. 1.

In Fig. 1b, the formation enthalpies per surface area of the important surface species hydrogen and hydroxyl are plotted. As recently discussed [16], in the potential range $0.5 < U < 0.75\,\mathrm{V}$, the so-called double-layer region, clean Pt(111) is thermodynamically stable , i.e., the Pt(111) electrode is not covered by any specifically adsorbed species. This means that hydrogen atoms on the electrode created through dehydrogenation reactions will readily be transfered into the electrolyte, thus prohibiting backward hydrogenation reactions. Aqueous water molecules serve as the source for oxygen via the water dissociation into adsorbed hydrogen and hydroxyl. As surface oxygen is energetically less favorable than adsorbed hydroxyl at the Pt(111)/water interface [14], surface hydroxyl is supposed to take part in the reactions.

4 Energetics of reaction intermediates

As the elementary reaction steps, we take into account C-H and O-H bond breaking and C-O bond formation. All possible reaction intermediates based on this assumption are listed in Table 2 and plotted in Fig. 2 with respect to the selected chemical and electrochemical environments in presented Table 1.

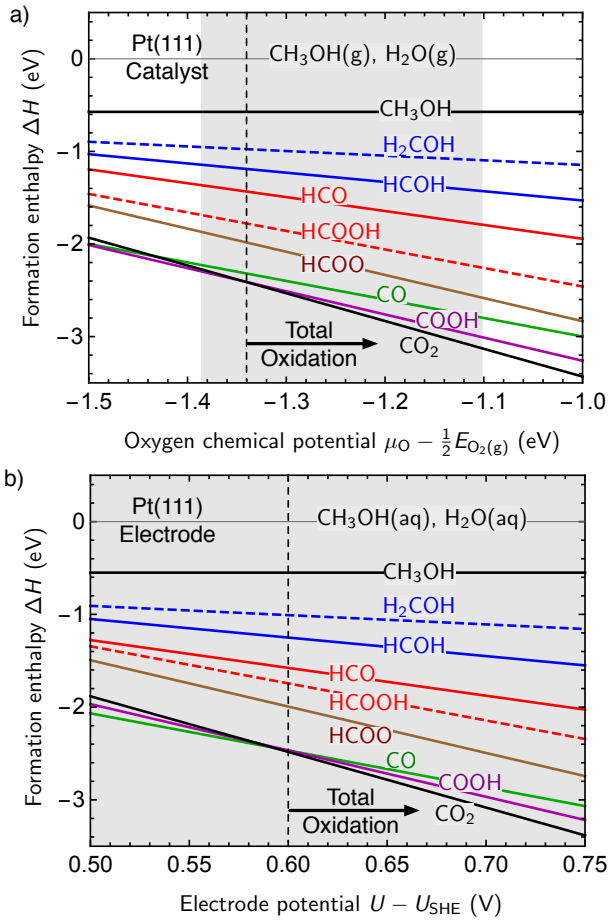

Fig. 2 Formation enthalpy of selected reaction intermediates in a) heterogeneous catalysis and b) electrocatalysis. The vertical dashed lines represent the chemical potential where CO_2 becomes the most favored species.

For both environments, gas phase and water, CO_2 is not the energetically most favorable product at the lower limit of the chemical potentials, but it only becomes the most stable adsorbed species at $\mu_O = -1.34\,\text{eV}$ with respect to oxygen gas in heterogeneous catalysis and at $U = 0.6\,\text{V}$ with respect to the standard hydrogen electrode in electrocatalysis. Note that the reported values for the standard electrode potential of the total electro-oxidation of methanol are 0.02 V [61] and 0.032 V [62], whereas we find a value of 0.24 V in water described as an implicit solvent [16]. Note furthermore that the gas phase chemical potential is a function of the partial pressure and temperature, i.e., any given chemical potential corresponds to a range of combinations of these two quantities. A chemical potential of $\mu_O = -1.34\,\text{eV}$ can for example

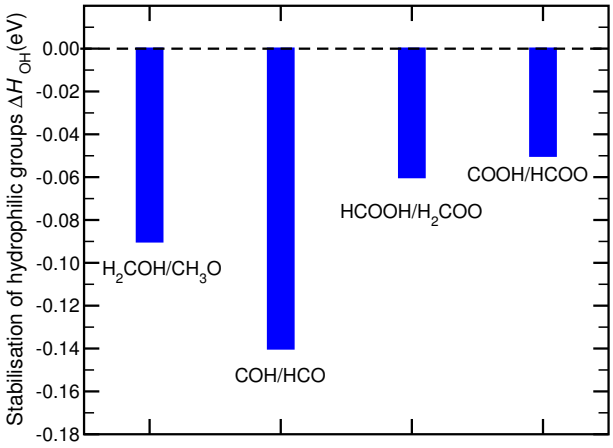

Fig. 3 Stabilization ΔH_{OH} of reaction intermediates in an aqueous electrolyte containing hydrophilic OH groups with respect to their isomers without OH groups determined according to Eq. 5.

been obtained by having a temperature of 700 K and a partial pressure of 25 μPa.

The presence of the aqueous environment does not change the adsorption energies dramatically. However, when we compare the formation enthalpies of reaction enthalpies of isomers such as methoxy (CH_3O) and hydroxymethyl (H_2COH) that have a common reference energy in the reservoir, we find that

Table 2 Formation enthalpies of reaction intermediates of methanol oxidation in heterogeneous catalysis and in electrocatalysis on clean Pt(111).

	Heterogeneous Catalysis		Electrocatalysis	
potential (eV):	$\mu_{\mathrm{O}} = -1.38$	$\mu_{\mathrm{O}} = -1.10$	$U = 0.50$	$U = 0.75$
CH_3OH	−0.57	−0.57	−0.55	−0.55
CH_3O	−0.12	−0.26	0.02	−0.23
H_2COH	−0.96	−1.10	−0.91	−1.16
$H_2C(OH)_2$	−1.10	−1.38	−0.83	−1.33
$HC(OH)_2$	−1.51	−1.93	−1.24	−1.99
CH_2O	−0.57	−0.85	−0.44	−0.94
COH	−1.63	−2.05	−1.68	−2.43
HCO	−1.37	−1.79	−1.28	−2.03
HCOH	−1.15	−1.43	−1.05	−1.55
H_2COO	−0.22	−0.78	0.20	−0.80
H_2COOH	−0.72	−1.14	−0.47	−1.22
HCOOH	−1.70	−2.26	−1.34	−2.34
HCOO	−1.88	−2.58	−1.49	−2.74
COOH	−2.31	−3.01	−1.97	−3.22
$C(OH)_2$	−2.03	−2.59	−1.86	−2.86
CO_{fcc}	−2.22	−2.78	−2.07	−3.07
CO_{top}	−2.24	−2.80	−2.07	−3.07
CO_2	−2.29	−3.13	−1.88	−3.38

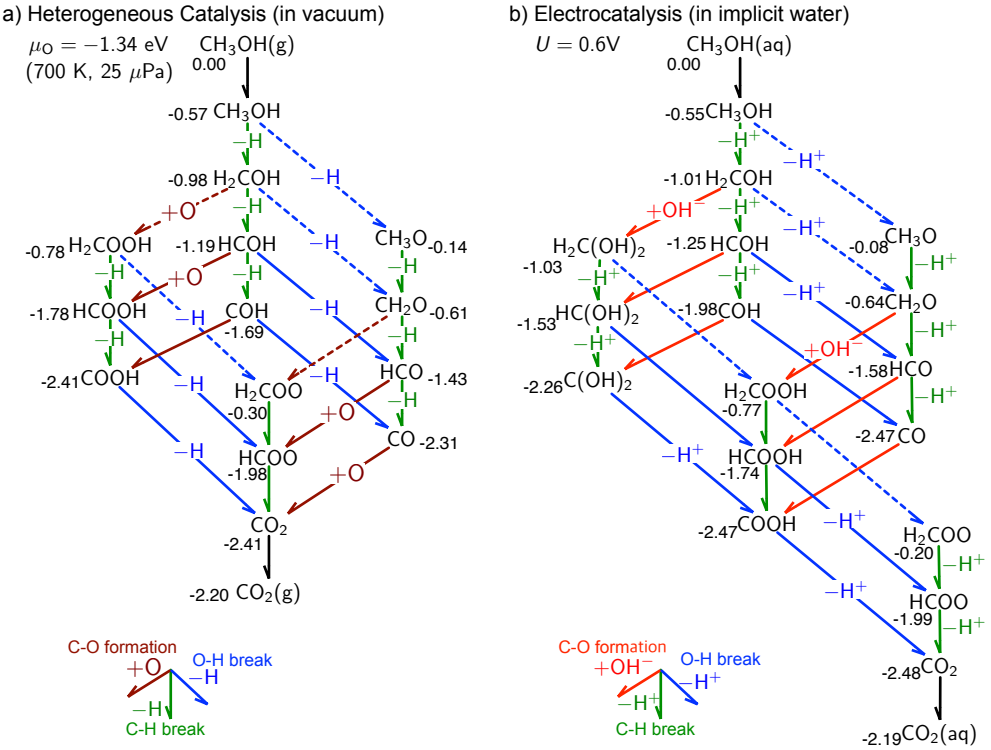

Fig. 4 Reaction paths of methanol oxidation a) in heterogeneous catalysis and b) in electrocatalysis.

species containing hydrophilic groups such as the hydroxyl group in H_2COH become more energetically stabilized in the aqueous environment which can be quantisized by evaluating

$$\Delta H_{\mathrm{OH}} = (\Delta H^{\mathrm{l}}(\mathrm{H_2COH}) - \Delta H^{\mathrm{l}}(\mathrm{CH_3O})) - (\Delta H^{\mathrm{g}}(\mathrm{H_2COH}) - \Delta H^{\mathrm{g}}(\mathrm{CH_3O}))\ , \tag{5}$$

where ΔH^{l} is the formation enthalpy according to Eq. 2 in the liquid phase appropriate for electrocatalysis and ΔH^{g} in the gas phase appropriate for heterogeneous catalysis. In fact, this significantly modifies the selectivity in the electrochemical environment compared to the gas-phase environment [16] and is in good agreement with a joint experimental-theoretical study of the methanol decomposition on platinum [67]. This additional stabilization through the presence of the hydroxyl group is also observed when comparing COH with HCO, HCOOH with H_2COO, and COOH with HCOO, as illustrated in Fig. 3 where the stabilisation ΔH_{OH} of reaction intermediates in the liquid phase is plotted for the four isomeric pairs mentioned above.

The reaction paths connecting the intermediates in heterogeneous catalysis and electrocatalysis are illustrated in Fig. 4. The main difference is that

OH is involved in C-O bond formation in electrocatalysis and atomic oxygen in heterogeneous catalysis. Consequently, an additional O-H bond breaking is required in electro-oxidation. Furthermore, the diol molecules having two hydroxyl groups can only be formed readily in electrocatalysis.

Under the conditions favorable for total oxidation described above, a higher oxidation number of the carbon species is associated with a larger formation enthalpy (see Table 2). As there is a range of chemical potentials at which CO_2 formation on clean Pt(111) is thermodynamically favorable, previous theoretical studies addressing the methanol oxidation in heterogeneous [63–66] and electrocatalysis [67–71] correctly captured the essentials of methanol total oxidation. However, methanol oxidation on clean Pt(111) does not correspond to the optimum situation. The oxidation will be more efficient in oxygen rich condition in which the catalyst becomes oxygen- or hydroxyl-covered [57].

We stress that a meaningful comparison of the results of first-principles calculations with experiment can only be done when the appropriate chemical environment is taken into account in the calculations. For example, the mass spectroscopy experiments by Reichert et al. [72, 40] demonstrated that the CO_2 formation from methanol and the decrease of the amount of adsorbed CO start at 0.6 V (see Fig. 6 of Ref. [40]). This corresponds to the regime in which the clean Pt(111) electrode is the most stable surface termination. Hence the formation enthalpies shown in Fig. 2b are suitable to describe the experimental situation. When we assume that the energetically mostly stable species exists dominantly on the electrode, the crossover of the largest formation enthalpy from CO to CO_2 in Fig. 2b is directly comparable to the experimental findings. To illustrate the importance of the proper consideration of the chemical environment, let us use the formation enthalpies of the reaction intermediates derived from the DFT calculations in vacuum for the electrocatalytic situation. Then, CO_2 becomes the most favorable reaction product already at an electrode potential of 0.52 V which corresponds to a down-shift of about 0.1 V compared to the calculations taking the aqueous solvent into account, thus also reducing the agreement with the experiment.

Figure 4 summarizes the energetics of the reaction intermediates in methanol oxidation in heterogeneous and electrocatalysis with respect to gas phase methanol and solvated methanol, respectively. The oxygen gas phase reservoir is characterized by an oxygen chemical potential of $\mu_O = -1.34\,\mathrm{eV}$, whereas the energies of the intermediates in electrocatalysis are derived for an electrode potential of $U = 0.6\,\mathrm{V}$. The green and blue arrows represent C-H and O-H bond breaking reactions, respectively, while the brown and red arrows denote C-O bond formation by O and OH associations. The solid and dashed arrows indicate exothermic and endothermic reactions, respectively. In vacuum, the oxidation through HCOH proceeds via a sequence of exothermic reactions (see Fig. 4a). An analysis of the energetics indicates that CH_3O and CH_2O formation are not favorable. However, methoxy formation is kinetically accessible because of the comparable activation barriers of C-H and O-H bond breaking in vacuum [65, 16]. Thus, CO_2 can be formed either in the so-called

indirect mechanism involving adsorbed CO or in a direct mechanism from formic acid (HCOOH) [64,65].

In water, the electro-oxidation paths through HCOH consist of consecutive exothermic reaction steps (see Fig. 4b). However, due to the presence of aqueous electrolyte methoxy formation becomes kinetically hindered, as we demonstrated recently [16]. This result agrees well with the experimental finding of a predominant H_2COH formation at the water/Pt(111) interface [73].

The reaction schemes depicted in Fig. 4 rely on an efficient supply channel of oxygen species, but the mechanism has not been explicitly discussed yet. In heterogeneous catalysis, oxygen atoms are provided by the dissociative adsorption of O_2 molecules which is operative above 150 K [74–76].

However, in the reaction in the aqueous environment, oxygen species are supplied by the dissociation of water molecules. Since the water dissociation on Pt(111) is hindered by a relatively large activation barrier of 0.8 eV [77–79], the hydroxyl production will be a rate limiting step in the whole oxidation process. Without sufficient OH production, CO adsorbed on the electrode will be the dominant reaction product. In the experiments by Reichert et al. [72,40], below 0.6 V, CO is the only detectable surface species and no CO_2 formation occurs. This indicates that there is a need for an efficient water dissociation mechanism in order to supply hydroxyl, for example at step edges of Pt or small Ru particle dispersed on the electrode.

5 Hydrogen-covered Pt(111) electrode

Finally, we discuss the influence of the electrochemical environment beyond optimal operating conditions. As discussed in Section 3, below 0.5 V the total oxidation of methanol is thermodynamically not favorable. In addition, the Pt(111) electrode is covered by H atoms that are supplied by the protons in the electrolyte. Hence, we focus on a partial oxidation path to CO formation. Note that in heterogeneous catalysis adsorbed hydrogen originates from gas-phase H_2 molecules which still typically adsorb dissociatively on metal surfaces [80].

First we address the initial methanol adsorption on Pt(111) as a function of hydrogen coverage. At the saturation coverage of $\theta_H = 1$, methanol is placed on top of hydrogen layer, whereas for smaller hydrogen coverages methanol is put at one of the free Pt sites.

In Fig. 5a, the formation enthalpies of hydrogen and methanol co-adsorption on Pt(111) are plotted as a function of the electrode potential. Methanol adsorption on the fully H-saturated electrode (red line) is only stable below 0.36 V, whereas methanol replaces an adsorbed hydrogen atom above 0.36 V.

The calculations show that methanol molecule can replace a surface H atom only above 0.36 V. Below 0.36 V, on the H saturated Pt electrode, because of the weaker interaction the adsorbed methanol molecule is located about 1 Å further away from the surface than on the clean Pt electrode. Then, it becomes difficult to catalyze the initial step of the methanol electro-oxidation directly

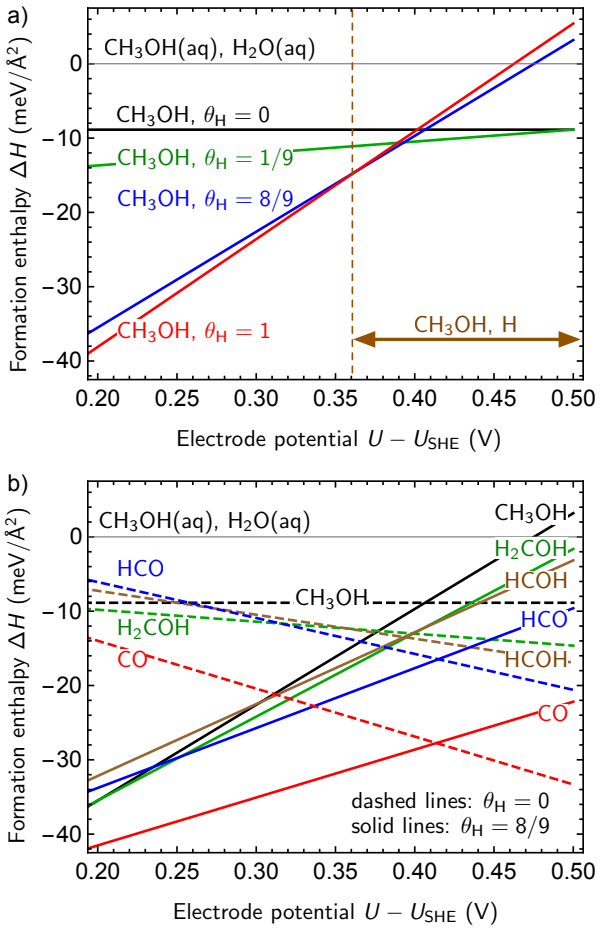

Fig. 5 a) Formation enthalpy per area of methanol on H-covered Pt(111) electrodes for various H coverages and b) formation enthalpy per area of the reaction intermediates on an H-covered electrode with $\theta_H = 8/9$. The concentration of the reaction intermediates on the electrode is 1/9 within a 3×3 surface unit cell.

by the Pt electrode, and CO formation from methanol will be slow and limited as observed in mass spectroscopy experiments [40].

In Fig. 5b, the formation enthalpies of the considered reaction intermediates are displayed for a hydrogen coverage of $\theta_H = 8/9$ (solid lines) and without any adsorbed hydrogen atoms (dashed lines). The adsorption of the reaction intermediates becomes more stable on clean Pt(111) than on H-covered Pt(111) at potentials above 0.4 V. Our calculations indicate that in the range $0.4 < U < 0.5$ V, the reaction intermediates in the methanol oxidation replace the adsorbed hydrogen atoms in a competitive fashion, similar to what has be adsorbed in the co-adsorption of halides and hydrogen [19,81]. Thus the

presence of methanol in the aqueous electrolyte even reduces the potential region in which so-called underpotential deposited (upd) hydrogen is stable on Pt(111).

Below 0.4 V, the reaction intermediates will be surrounded by adsorbed H atoms. Thus hydrogenation reactions reversing the oxidation become possible. Specifically, the formation of H_2COH (solid green line) becomes more favorable than HCOH formation (solid brown line) below 0.4 V which means that the hydrogenation of HCOH becomes exothermic. Then, this oxidation step will hinder the further progress of the partial oxidation of methanol significantly and will be responsible for a low efficiency towards CO formation.

6 Conclusion

Using a grand-canonical approach, we have addressed methanol oxidation on Pt(111), both in a situation corresponding to heterogeneous catalysis at the solid-gas interface as well as for a electrocatalytic environment at the solid-water interface. The aqueous electrolyte has been taken into account within an implicit solvent model. Thus we have identified characteristic differences between the methanol oxidation paths in heterogeneous and electro-catalysis. The presence of the aqueous electrolyte leads to the stabilization of reaction intermediates that contain hydrophilic groups such as hydroxyl when isomers are compared. This also modifies the selectivitiy of the methanol oxidation in heterogeneous compared to electro-catalysis.

Furthermore, we have addressed the partial oxidation of methanol on H-covered Pt electrodes corresponding to a situation of low electrode potentials. The presence of adsorbed hydrogen atoms on Pt(111) is shown to be detrimental for the methanol oxidation.

Acknowledgement

This research has been supported by the German Research Foundation (DFG) through contract GR 1503/21-2. The authors acknowledge the computer time supported by the state of Baden-Württemberg through the bwHPC project and the Germany Research Foundation (DFG) through grant number INST 40/467-1 FUGG.

References

1. R. Schlögl, The role of chemistry in the energy challenge. ChemSusChem **3**, 209 (2010)
2. C. Hartnig, P. Vassilev, M.T.M. Koper, *Ab initio* and classical molecular dynamics studies of electrode reactions. Electrochim. Acta **48**, 3751 (2003)
3. C. Hartnig, E. Spohr, The role of water in the initial steps of methanol oxidation on Pt(111). Chem. Phys. **319**, 185 (2005)
4. M.J. Janik, C.D. Taylor, M. Neurock, First principles analysis of the electrocatalytic oxidation of methanol and carbon monoxide. Top. Catal. **46**, 306 (2007). DOI 10.1007/s11244-007-9004-9

5. J.A. Keith, T. Jacob, Theoretical studies of potential-dependent and competing mechanisms of the electrocatalytic oxygen reduction reaction on Pt(111). Angew. Chem. Int. Ed. **49**, 9521 (2010). DOI 10.1002/anie.201004794
6. F. Calle-Vallejo, M.T. Koper, First-principles computational electrochemistry: Achievements and challenges. Electrochim. Acta **84**(0), 3 (2012). DOI http://dx.doi.org/10.1016/j.electacta.2012.04.062
7. P. Quaino, E. Santos, H. Wolfschmidt, M. Montero, U. Stimming, Theory meets experiment: Electrocatalysis of hydrogen oxidation/evolution at Pd-Au nanostructures. Catal. Today **177**, 55 (2011). DOI 10.1016/j.cattod.2011.05.004
8. P. Quaino, N. Luque, G. Soldano, R. Nazmutdinov, E. Santos, T. Roman, A. Lundin, A. Groß, W. Schmickler, Solvated protons in density functional theory - a few examples. Electrochim. Acta **105**, 248 (2013)
9. K. Chan, J.K. Nørskov, Electrochemical barriers made simple. J. Phys. Chem. Lett. **6**(14), 2663 (2015). DOI 10.1021/acs.jpclett.5b01043
10. A. Groß, F. Gossenberger, X. Lin, M. Naderian, S. Sakong, T. Roman, Water structures at metal electrodes studied by ab initio molecular dynamics simulations. J. Electrochem. Soc. **161**(8), E3015 (2014). DOI 10.1149/2.003408jes
11. T. Roman, F. Gossenberger, K. Forster-Tonigold, A. Groß, Halide adsorption on close-packed metal electrodes. Phys. Chem. Chem. Phys. **16**, 13630 (2014). DOI 10.1039/C4CP00237G
12. F. Gossenberger, T. Roman, K. Forster-Tonigold, A. Groß, Change of the work function of platinum electrodes induced by halide adsorption. Beilstein J. Nanotechnol. **5**, 152 (2014). DOI 10.3762/bjnano.5.15
13. N.G. Hörmann, M. Jäckle, F. Gossenberger, T. Roman, K. Forster-Tonigold, M. Naderian, S. Sakong, A. Groß, Some challenges in the first-principles modeling of structures and processes in electrochemical energy storage and transfer. J. Power Sources **275**, 531 (2015). DOI http://dx.doi.org/10.1016/j.jpowsour.2014.10.198
14. S. Sakong, M. Naderian, K. Mathew, R.G. Hennig, A. Groß, Density functional theory study of the electrochemical interface between a Pt electrode and an aqueous electrolyte using an implicit solvent method. J. Chem. Phys. **142**(23), 234107 (2015). DOI http://dx.doi.org/10.1063/1.4922615
15. F. Gossenberger, T. Roman, A. Groß, Equilibrium coverage of halides on metal electrodes. Surf. Sci. **631**, 17 (2015). DOI http://dx.doi.org/10.1016/j.susc.2014.01.021
16. S. Sakong, A. Groß, The Importance of the Electrochemical Environment in the Electro-Oxidation of Methanol on Pt(111). ACS Catal. **6**, 5575 (2016). DOI 10.1021/acscatal.6b00931
17. S. Sakong, K. Forster-Tonigold, A. Groß, The structure of water at a Pt(111) electrode and the potential of zero charge studied from first principles. J. Chem. Phys. **144**(19), 194701 (2016). DOI http://dx.doi.org/10.1063/1.4948638
18. X. Lin, F. Evers, A. Groß, First-principles study of the structure of water layers on flat and stepped Pb electrodes. Beilstein J. Nanotechnol. **7**, 533 (2016). DOI 10.3762/bjnano.7.47
19. F. Gossenberger, T. Roman, A. Groß, Hydrogen and halide co-adsorption on Pt(111) in an electrochemical environment: a computational perspective. Electrochim. Acta **216**, 152 (2016). DOI http://dx.doi.org/10.1016/j.electacta.2016.08.117
20. M. Mehlhorn, S. Schnur, A. Groß, K. Morgenstern, Molecular-scale imaging of water near charged surfaces. ChemElectroChem **1**(2), 431 (2014). DOI 10.1002/celc.201300063
21. S. Schnur, A. Groß, Properties of metal–water interfaces studied from first principles. New J. Phys. **11**(12), 125003 (2009). DOI 10.1088/1367-2630/11/12/125003
22. S. Schnur, A. Groß, Challenges in the first-principles description of reactions in electrocatalysis. Catal. Today **165**(1), 129 (2011). DOI 10.1016/j.cattod.2010.11.071
23. A. Ignaczak, R. Nazmutdinov, A. Goduljan, L.M. de Campos Pinto, F. Juarez, P. Quaino, E. Santos, W. Schmickler, A scenario for oxygen reduction in alkaline media. Nano Energy **26**, 558 (2016). DOI http://dx.doi.org/10.1016/j.nanoen.2016.06.001
24. C. Hartnig, M.T.M. Koper, Solvent reorganization in electron and ion transfer reactions near a smooth electrified surface: a molecular dynamics study. J. Am. Chem. Soc. **125**, 9840 (2003)
25. K. Reuter, D. Frenkel, M. Scheffler, The steady state of heterogeneous catalysis, studied by first-principles statistical mechanics. Phys. Rev. Lett. **93**, 116105 (2004)

26. K. Reuter, M. Scheffler, First-principles kinetic monte carlo simulations for heterogeneous catalysis: Application to the CO oxidation at RuO_2(110). Phys. Rev. B **73**, 045433 (2006)
27. J. Rogal, K. Reuter, M. Scheffler, CO oxidation at Pd(100): A first-principles constrained thermodynamics study. Phys. Rev. B **75**, 205433 (2007). DOI 10.1103/PhysRevB.75.205433
28. C. Shi, H.A. Hansen, A.C. Lausche, J.K. Norskov, Trends in electrochemical co2 reduction activity for open and close-packed metal surfaces. Phys. Chem. Chem. Phys. **16**, 4720 (2014). DOI 10.1039/C3CP54822H
29. J.K. Nørskov, J. Rossmeisl, A. Logadottir, L. Lindqvist, J.R. Kitchin, T. Bligaard, H. Jónsson, Origin of the overpotential for oxygen reduction at a fuel-cell cathode. J. Phys. Chem. B **108**(46), 17886 (2004). DOI 10.1021/jp047349j
30. E. Skulason, G.S. Karlberg, J. Rossmeisl, T. Bligaard, J. Greeley, H. Jonsson, J.K. Norskov, Density functional theory calculations for the hydrogen evolution reaction in an electrochemical double layer on the Pt(111) electrode. Phys. Chem. Chem. Phys. **9**, 3241 (2007). DOI 10.1039/B700099E
31. J.K. Nørskov, F. Abild-Pedersen, F. Studt, T. Bligaard, Density functional theory in surface chemistry and catalysis. Proceedings of the National Academy of Sciences **108**(3), 937 (2011). DOI 10.1073/pnas.1006652108
32. A.R. Leach, *Molecular Modelling: Principles and Applications*, 2nd edn. (Pearson, Harlow, 2001)
33. A. Roudgar, A. Groß, Water bilayer on the Pd/Au(111) overlayer system: coadsorption and electric field effects. Chem. Phys. Lett. **409**, 157 (2005)
34. A. Michaelides, Density functional theory simulations of water-metal interfaces: Waltzing waters, a novel 2D ice phase, and more. Appl. Phys. A **85**, 415 (2006)
35. D. Gunceler, K. Letchworth-Weaver, R. Sundararaman, K.A. Schwarz, T.A. Arias, The importance of nonlinear fluid response in joint density-functional theory studies of battery systems. Model. Simul. Mater. Sc. **21**(7), 074005 (2013). DOI 10.1088/0965-0393/21/7/074005
36. K. Letchworth-Weaver, T.A. Arias, Joint density functional theory of the electrode-electrolyte interface: Application to fixed electrode potentials, interfacial capacitances, and potentials of zero charge. Phys. Rev. B **86**, 075140 (2012). DOI 10.1103/PhysRevB.86.075140
37. S.A. Petrosyan, A.A. Rigos, T.A. Arias, Joint density-functional theory: ab initio study of cr2o3 surface chemistry in solution. J. Phys. Chem. B **109**(32), 15436 (2005). DOI 10.1021/jp044822k
38. S.A. Petrosyan, J.F. Briere, D. Roundy, T.A. Arias, Joint density-functional theory for electronic structure of solvated systems. Phys. Rev. B **75**, 205105 (2007). DOI 10.1103/PhysRevB.75.205105
39. A. Arico, V. Baglio, A.D. Blasi, E. Modica, P. Antonucci, V. Antonucci, Analysis of the high-temperature methanol oxidation behaviour at carbon-supported ptru catalysts. J. Electroanal. Chem. **557**, 167 (2003). DOI http://dx.doi.org/10.1016/S0022-0728(03)00369-3
40. R. Reichert, J. Schnaidt, Z. Jusys, R.J. Behm, The influence of reactive side products on the electrooxidation of methanol - a combined in situ infrared spectroscopy and online mass spectrometry study. Phys. Chem. Chem. Phys. **16**, 13780 (2014). DOI 10.1039/C4CP01229A
41. G. Kresse, J. Furthmüller, Efficient iterative schemes for ab initio total-energy calculations using a plane-wave basis set. Phys. Rev. B **54**, 11169 (1996). DOI 10.1103/PhysRevB.54.11169
42. B. Hammer, L.B. Hansen, J.K. Nørskov, Improved adsorption energetics within density-functional theory using revised Perdew-Burke-Ernzerhof functionals. Phys. Rev. B **59**, 7413 (1999)
43. S. Grimme, J. Antony, S. Ehrlich, H. Krieg, A consistent and accurate ab initio parametrization of density functional dispersion correction (dft-d) for the 94 elements h-pu. J. Chem. Phys. **132**(15), 154104 (2010). DOI http://dx.doi.org/10.1063/1.3382344
44. S. Grimme, Density functional theory with london dispersion corrections. Wiley Interdiscip. Rev. Comput. Mol. Sci. **1**(2), 211 (2011). DOI 10.1002/wcms.30

45. S. Grimme, A. Hansen, J.G. Brandenburg, C. Bannwarth, Dispersion-corrected mean-field electronic structure methods. Chem. Rev. **116**(9), 5105 (2016). DOI 10.1021/acs.chemrev.5b00533
46. K. Tonigold, A. Groß, Dispersive interactions in water bilayers at metallic surfaces: A comparison of the pbe and rpbe functional including semiempirical dispersion corrections. J. Comput. Chem. **33**(6), 695 (2012). DOI 10.1002/jcc.22900
47. K. Forster-Tonigold, A. Groß, Dispersion corrected rpbe studies of liquid water. J. Chem. Phys. **141**, 064501 (2014). DOI http://dx.doi.org/10.1063/1.4892400
48. B. Koslowski, A. Tschetschetkin, N. Maurer, P. Ziemann, J. Kučera, A. Groß, 4,4'-dithiodipyridine on Au(111): a combined STM, STS, and DFT study. J. Phys. Chem. C **117**, 20060 (2013)
49. K. Mathew, R. Sundararaman, K. Letchworth-Weaver, T.A. Arias, R.G. Hennig, Implicit solvation model for density-functional study of nanocrystal surfaces and reaction pathways. J. Chem. Phys. **140**, 084106 (2014). DOI http://dx.doi.org/10.1063/1.4865107
50. P.E. Blöchl, Projector augmented-wave method. Phys. Rev. B **50**, 17953 (1994). DOI 10.1103/PhysRevB.50.17953
51. G. Mercurio, E.R. McNellis, I. Martin, S. Hagen, F. Leyssner, S. Soubatch, J. Meyer, M. Wolf, P. Tegeder, F.S. Tautz, K. Reuter, Structure and energetics of azobenzene on ag(111): Benchmarking semiempirical dispersion correction approaches. Phys. Rev. Lett. **104**, 036102 (2010). DOI 10.1103/PhysRevLett.104.036102
52. M. Fishman, H.L. Zhuang, K. Mathew, W. Dirschka, R.G. Hennig, Accuracy of exchange-correlation functionals and effect of solvation on the surface energy of copper. Phys. Rev. B **87**, 245402 (2013). DOI 10.1103/PhysRevB.87.245402
53. O. Andreussi, I. Dabo, N. Marzari, Revised self-consistent continuum solvation in electronic-structure calculations. J. Chem. Phys. **136**(6), 064102 (2012). DOI http://dx.doi.org/10.1063/1.3676407
54. O. Andreussi, N. Marzari, Electrostatics of solvated systems in periodic boundary conditions. Phys. Rev. B **90**, 245101 (2014). DOI 10.1103/PhysRevB.90.245101
55. S. Günther, L. Zhou, M. Hävecker, A. Knop-Gericke, E. Kleimenov, R. Schlögl, R. Imbihl, Adsorbate coverages and surface reactivity in methanol oxidation over Cu(110): A in situ photoelectron spectroscopy study. J. Chem. Phys. **125**, 114709 (2006)
56. S. Sakong, A. Groß, Density functional theory study of the partial oxidation of methanol on copper surfaces. J. Catal. **231**, 420 (2005). DOI 10.1016/j.jcat.2005.02.009
57. S. Sakong, A. Groß, Total oxidation of methanol on Cu(110): a density functional theory study. J. Phys. Chem. A **111**, 8814 (2007). DOI 10.1021/jp072773g
58. W. Greiner, L. Neise, H. Stöcker, *Thermodynamik und Statistische Mechanik* (Harri Deutsch, Frankfurt am Main, 1987)
59. S. Sakong, Y.A. Du, P. Kratzer, Interface defects and impurities at the growth zone of Au-catalyzed GaAs nanowire from first principles. Phys. Status Solidi Rapid Res. Lett. **7**(10), 882 (2013). DOI 10.1002/pssr.201307210
60. K. Reuter, M. Scheffler, Composition, structure, and stability of RuO_2(110) as a function of oxygen pressure. Phys. Rev. B **65**, 035406 (2001). DOI 10.1103/PhysRevB.65.035406
61. T. Iwasita, Electrocatalysis of methanol oxidation. Electrochim. Acta **47**(22–23), 3663 (2002). DOI http://dx.doi.org/10.1016/S0013-4686(02)00336-5
62. A.B. Anderson, H.A. Asiri, Reversible potentials for steps in methanol and formic acid oxidation to CO_2; adsorption energies of intermediates on the ideal electrocatalyst for methanol oxidation and CO_2 reduction. Phys. Chem. Chem. Phys. **16**, 10587 (2014). DOI 10.1039/C3CP54837F
63. F. Calle-Vallejo, J. Tymoczko, V. Colic, Q.H. Vu, M.D. Pohl, K. Morgenstern, D. Loffreda, P. Sautet, W. Schuhmann, A.S. Bandarenka, Finding optimal surface sites on heterogeneous catalysts by counting nearest neighbors. Science **350**(6257), 185 (2015). DOI 10.1126/science.aab3501
64. J. Greeley, M. Mavrikakis, A first-principles study of methanol decomposition on Pt(111). J. Am. Chem. Soc. **124**, 7193 (2002)
65. J. Greeley, M. Mavrikakis, Competitive paths for methanol decomposition on Pt(111). J. Am. Chem. Soc. **126**, 3910 (2004). DOI 10.1021/ja037700z

66. S.K. Desai, M. Neurock, K. Kourtakis, A periodic density functional theory study of the dehydrogenation of methanol over Pt(111). J. Phys. Chem. B **106**(10), 2559 (2002). DOI 10.1021/jp0132984
67. D. Cao, G.Q. Lu, A. Wieckowski, S.A. Wasileski, M. Neurock, Mechanisms of methanol decomposition on platinum: a combined experimental and ab initio approach. J. Phys. Chem. B **109**(23), 11622 (2005). DOI 10.1021/jp0501188
68. C.D. Taylor, S.A. Wasileski, J.S. Filhol, M. Neurock, First principles reaction modeling of the electrochemical interface: Consideration and calculation of a tunable surface potential from atomic and electronic structure. Phys. Rev. B **73**, 165402 (2006). DOI 10.1103/PhysRevB.73.165402
69. H.F. Wang, Z.P. Liu, Formic acid oxidation at Pt/H_2O interface from periodic DFT calculations integrated with a continuum solvation model. J. Phys. Chem. C **113**(40), 17502 (2009). DOI 10.1021/jp9059888
70. Y.H. Fang, Z.P. Liu, Tafel kinetics of electrocatalytic reactions: From experiment to first-principles. ACS Catal. **4**(12), 4364 (2014). DOI 10.1021/cs501312v
71. Y.H. Fang, Z.P. Liu, First principles tafel kinetics of methanol oxidation on Pt(111). Surf. Sci. **631**, 42 (2015). DOI http://dx.doi.org/10.1016/j.susc.2014.05.014
72. R. Reichert, J. Schnaidt, Z. Jusys, R.J. Behm, The influence of reactive side products in electrocatalytic reactions: Methanol oxidation as case study. ChemPhysChem **14**(16), 3678 (2013). DOI 10.1002/cphc.201300726
73. K. Franaszczuk, E. Herrero, P. Zelenay, A. Wieckowski, J. Wang, R.I. Masel, A comparison of electrochemical and gas-phase decomposition of methanol on platinum surfaces. J. Phys. Chem. **96**(21), 8509 (1992). DOI 10.1021/j100200a056
74. J. Wintterlin, R. Schuster, G. Ertl, Existence of a "hot" atom mechanism for the dissociation of O_2 on Pt(111). Phys. Rev. Lett. **77**, 123 (1996)
75. A. Eichler, J. Hafner, Molecular precursors in the dissociative adsorption of O_2 on Pt(111). Phys. Rev. Lett. **79**, 4481 (1997). DOI 10.1103/PhysRevLett.79.4481
76. A. Groß, A. Eichler, J. Hafner, M.J. Mehl, D.A. Papaconstantopoulos, *Ab initio* based tight-binding molecular dynamics simulation of the sticking and scattering of O_2/Pt(111). J. Chem. Phys. **124**, 174713 (2006)
77. L.C. Grabow, A.A. Gokhale, S.T. Evans, J.A. Dumesic, M. Mavrikakis, Mechanism of the water gas shift reaction on Pt: First principles, experiments, and microkinetic modeling. J. Phys. Chem. C **112**(12), 4608 (2008). DOI 10.1021/jp7099702
78. E.M. Karp, C.T. Campbell, F. Studt, F. Abild-Pedersen, J.K. Nørskov, Energetics of oxygen adatoms, hydroxyl species and water dissociation on Pt(111). J. Phys. Chem. C **116**(49), 25772 (2012). DOI 10.1021/jp3066794
79. J.C. Fajín, M.N. D. S. Cordeiro, J.B. Gomes, Density functional theory study of the water dissociation on platinum surfaces: General trends. J. Phys. Chem. A **118**(31), 5832 (2014). DOI 10.1021/jp411500j
80. A. Groß, Dynamical quantum processes of molecular beams at surfaces: dissociative adsorption of hydrogen on metal surfaces. Surf. Sci. **363**, 1 (1996)
81. X. Lin, F. Gossenberger, A. Groß, Ionic adsorbate structures on metal electrodes calculated from first-principles. Ind. Eng. Chem. Res. **55**(42), 11107 (2016). DOI 10.1021/acs.iecr.6b03087